AD

TECHNICAL REPORT ARCCB-TR-03003

CRITICAL FRACTURE PROCESSES IN ARMY CANNONS: A REVIEW

JOHN H. UNDERWOOD
EDWARD TROIANO

MARCH 2003

US ARMY ARMAMENT RESEARCH,
DEVELOPMENT AND ENGINEERING CENTER
Close Combat Armaments Center
Benét Laboratories
Watervliet, NY 12189-4000

DISCLAIMER

The findings in this report are not to be construed as an official Department of the Army position unless so designated by other authorized documents.

The use of trade name(s) and/or manufacturer(s) does not constitute an official endorsement or approval.

DESTRUCTION NOTICE

For classified documents, follow the procedures in DoD 5200.22-M, Industrial Security Manual, Section II-19, or DoD 5200.1-R, Information Security Program Regulation, Chapter IX.

For unclassified, limited documents, destroy by any method that will prevent disclosure of contents or reconstruction of the document.

For unclassified, unlimited documents, destroy when the report is no longer needed. Do not return it to the originator.

REPORT DOCUMENTATION PAGE

Form Approved
OMB No. 0704-0188

1. AGENCY USE ONLY *(Leave Blank)*	2. REPORT DATE March 2003	3. REPORT TYPE AND DATES COVERED Final

4. TITLE AND SUBTITLE
CRITICAL FRACTURE PROCESSES
IN ARMY CANNONS: A REVIEW

5. FUNDING NUMBERS
AMCMS No. 6226.24.H180.0
PRON No. TU2

6. AUTHORS
John H. Underwood and Edward Troiano

7. PERFORMING ORGANIZATION NAME(S) AND ADDRESS(ES)
U.S. Army ARDEC
Benet Laboratories, AMSTA-AR-CCB-O
Watervliet, NY 12189-4000

8. PERFORMING ORGANIZATION REPORT NUMBER
ARCCB-TR-03003

9. SPONSORING / MONITORING AGENCY NAME(S) AND ADDRESS(ES)
U.S. Army ARDEC
Close Combat Armaments Center
Picatinny Arsenal, NJ 07806-5000

10. SPONSORING / MONITORING AGENCY REPORT NUMBER

11. SUPPLEMENTARY NOTES
Presented at Gun Tubes Conference 2002, Keble College, Oxford, UK, 15-18 September 2002.
Published in *Journal of Pressure Vessel Technology*.

12a. DISTRIBUTION / AVAILABILITY STATEMENT
Approved for public release; distribution unlimited.

12b. DISTRIBUTION CODE

13. ABSTRACT *(Maximum 200 words)*
Fast fracture in cannons can well be described using elastic-plastic fracture toughness, in combination with comparisons of cannon section size relative to the size required to maintain plane-strain fracture. *Fatigue fracture* of cannon tubes is modeled from results of full-size fatigue tests that simulate cannon firing. These tests are also the basis of fatigue-intensity-factor modeling of fatigue life, which incorporates material strength, initial crack size, and Bauschinger-modified autofrettage residual stress into life predictions. *Environment-assisted fracture* in the thermally damaged near-bore region of fired cannons is shown to be controlled by hydrogen. High-strength cannon steels are susceptible to hydrogen; cannon propellant gases provide the hydrogen; and the source of sustained tensile stress is the near-bore thermal damage and compressive yielding. A thermomechanical model predicts tensile residual stress of similar depth to that of observed hydrogen cracks. *Coating fracture* in the thermal-damage region of fired cannons is characterized and modeled. The Evans/Hutchinson slip-zone concept is extended to calculate in-situ coating fracture strength from observed crack spacing and hardness in the damaged region.

14. SUBJECT TERMS
Cannons, Fast Fracture, Fatigue Fracture,
Environment-Assisted Fracture, Coating Fracture

15. NUMBER OF PAGES
20

16. PRICE CODE

17. SECURITY CLASSIFICATION OF REPORT	18. SECURITY CLASSIFICATION OF THIS PAGE	19. SECURITY CLASSIFICATION OF ABSTRACT	20. LIMITATION OF ABSTRACT
UNCLASSIFIED	UNCLASSIFIED	UNCLASSIFIED	UL

TABLE OF CONTENTS

TABLES

LIST OF ILLUSTRATIONS

ACKNOWLEDGEMENTS

The authors are pleased to acknowledge the help of C. Rickard, C. Mossey, K. Olsen, P. J. Cote, and M. E. Todaro of Benet Laboratories for conducting much of the experimental characterization described here.

INTRODUCTION

An interesting variety of fracture processes have been observed in U.S. Army cannons during the past four decades. This report describes these processes in a brief chronological summary and outlines the experimental and analytical methods currently used to address the various types of fracture in cannons. Each of three fundamental fracture processes—fast, fatigue, and environment-assisted fracture—has been a critical problem with cannons at some point in time. Also recently, fracture of bore protective coatings has raised concern, possibly involving each of the three types of fracture. The emphasis here will be the fracture problems that are still important with today's cannons and the current solutions to these problems, with limited descriptions of earlier work. Table 1 summarizes the current critical fracture problems and solutions that will be reviewed.

Table 1. Critical Fracture Problems in Army Cannons

Problem	Analysis	Experiment
Fast Fracture	Elastic-Plastic Fracture Mechanics	J_{Ic} Fracture Toughness
Fatigue Fracture	*Fatigue Intensity Factor* Versus Measured Life	Safe Life Fatigue Tests
Environmental Fracture	Thermomechanical Model	*da/dt* Versus Applied *K*
Coating Fracture	Interface Slip Model	Metallographic Section of Thermal Damage

Fast fracture of cannons will be discussed in relation to an early brittle fracture of a cannon and the poor fracture toughness of steels of that time, contrasted to current lower-strength, higher-toughness gun steel. Plastic zone analyses will be used to show important differences in fast fracture behavior with steel strength level and with test specimen versus gun tube configuration.

Fatigue fracture behavior of cannons will be summarized using a range of early and current results, so that the important effect of autofrettage can be demonstrated over a wide range of control parameters for fatigue. Examples will be shown of the log-normal method for determining experimental safe fatigue life and the fatigue-intensity-factor method for describing mean fatigue life, including Bauschinger effects.

Environmental fracture of cannons, particularly in the near-bore thermally damaged region, has greatly increased in importance in recent years, due to higher and more prolonged cannon gas temperatures. Since a bore coating in most modern cannon tubes protects the near-bore region, environmental fracture and coating fracture have become significantly interconnected in cannons. A thermomechanical model describing near-bore temperatures, stresses, and crack depth will be summarized, including a new modification to account for steel

transformational stress. Results will be shown from a solid mechanics model of coating fracture, concentrating on the coating residual stresses that cause fracture in the near-bore thermally yielded region.

FAST FRACTURE

An Early Failure

An unanticipated battlefield failure of a 175-mm inner diameter (ID) cannon tube in 1966 (ref 1) focused attention on fast fracture of Army cannons. The strength, fracture toughness, and chemical composition of the failed tube are contrasted in Table 2 with like information for current cannons. The 74 MPa $m^{1/2}$ toughness of the failed tube was below the 88 MPa $m^{1/2}$ average toughness of other early tubes, but the strength and composition are typical of the early 175-mm tubes. The fracture surface of the failed tube is shown as Figure 1. Note the semi-elliptically shaped, 10-mm deep crack at the top-center of the photo. A crack this size, combined with the tensile stress at the tube ID due to the firing pressure gave an applied stress intensity of 99 MPa $m^{1/2}$, well above the toughness, so fast fracture was expected.

Table 2. Properties of A723 Steel Used for Cannon Tubes

	Yield Strength (MPa)	Fracture Toughness (MPa $m^{1/2}$)	Chemical Composition (Weight %)				
			Ni	Cr	Mo	C	S
Failed Tube: 175-mm	1180	74	1.8	1.2	0.68	0.36	0.008
Current Tubes: 120-mm	1100	140	3.1	1.1	0.54	0.33	0.003

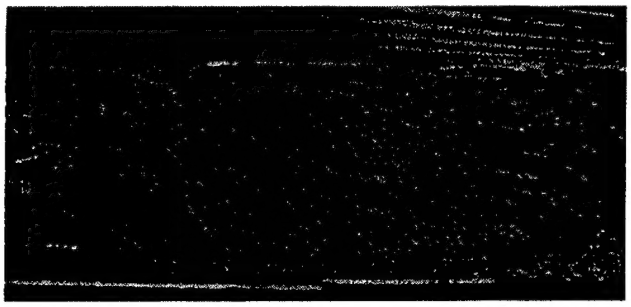

Figure 1. Fracture surface of a 175-mm cannon tube.

The steel currently used for cannon tubes is a remelted ASTM A723 Grade 2, Ni-Cr-Mo-V steel. Referring again to Table 2, the steel is characterized by a lower yield strength, typically about 1100 MPa, and a significantly increased fracture toughness. The increased toughness is due to the lower strength, the remelt process, and the higher nickel content and the lower sulfur content. A graphic display of the improved resistance to fast fracture of the current cannon tube

steel is shown in Figure 2, which depicts load-displacement plots from fracture toughness tests using the standard ASTM method (ref 2). The test of current tube steel was an unloading-compliance J_{Ic} test, in which the load is reduced at a number of points in order to measure the specimen compliance and thereby determine the amount of crack growth that has occurred. Note that the current steel sustained considerable load and permanent displacement before being unloaded with no final failure having occurred. In contrast, the plot of the failed tube material, reproduced here from the early results, shows abrupt and complete fracture with no measurable permanent displacement. It is clear that the current cannon tube steel has greatly increased resistance to fast fracture than the early steel that sustained a brittle, fast fracture.

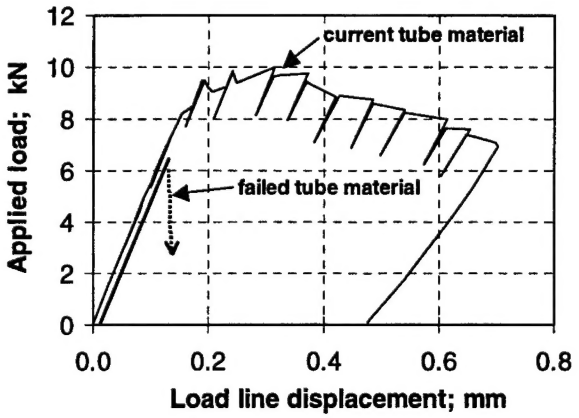

Figure 2. Fracture toughness tests of cannon steel.

The ASTM compliance-unloading J_{Ic} fracture toughness test (ref 2) is the critical material property test that is currently used in both manufacturing quality assurance tests of cannon steel and in development of new cannons. However, due to the complexity and high cost of the J_{Ic} test, the Charpy V-notch impact energy test (ref 3) is used as a simpler correlative test, once the J_{Ic} fracture toughness of a given cannon steel has been established.

Yielding Analyses

The improved toughness of cannon steel at lower yield strength, discussed above, has been carefully studied for many years and found to be critical to the understanding of fast fracture in cannons. Evaluation of actual or potential fast fracture in cannons always includes measurements of yield strength and fracture toughness. An Irwin plastic zone-size analysis of these measurements from a wide range of cannon steels in the 1000 to 1250 MPa strength range (ref 4) is shown in Figure 3. A parameter derived from the Irwin plastic zone concept is plotted versus yield strength, where the Irwin parameter is determined as

$$\textit{plane-strain size} = w/2 = 2.5(K_{Ic}/Y)^2 \qquad (1)$$

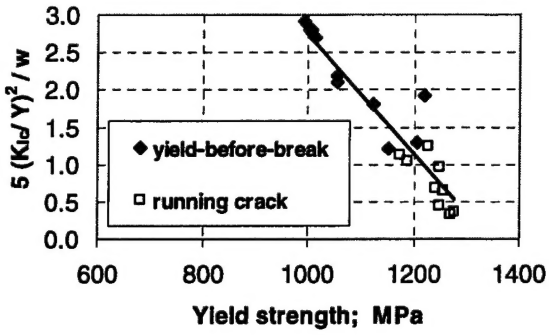

Figure 3. Effect of yield strength on fracture of cannons.

The quantity $2.5(K_{Ic}/Y)^2$ should be recognized (ref 2) as the size requirement for plane-strain conditions in a fracture toughness test. For a crack at the mid-wall position in a cannon tube, the critical plane-strain size is the dimension ahead or behind the crack tip, which is half the wall thickness, $w/2$. Thus, the $5(K_{Ic}/Y)^2/w$ parameter in Figure 3 gives an indication of whether or not plane-strain conditions control the failure of a cannon tube. For $5(K_{Ic}/Y)^2/w > 1$, plane-strain conditions are no longer dominant, because the plastic zone is large enough to modify the plane-strain conditions. Each of the data points in Figure 3 represents a hydraulically pressurized fatigue test of the breech section of a cannon. The final fatigue cycle resulted in a through-wall crack that in some cases became a running crack, traveling 100-mm or more down the tube axis. Note that $5(K_{Ic}/Y)^2/w = 1$ provides a useful separation between running cracks and those with what is called yield-before-break behavior. The results in Figure 3 show that an Irwin plastic zone analysis of strength and toughness properties can identify a critical yield strength, about 1200 MPa, above which fast fracture problems with cannon tubes become particularly critical. This type of yield-before-break analysis (ref 4) has particular applicability to vessels with $Y > 1000$ MPa, whereas traditional leak-before-break analysis of pressure vessels is appropriate for lower-strength steels. The basic difference between the two types of analysis is that yield-before-break involves a yielding-dominated delay in the final fast cracking failure out to the vessel outer diameter (OD), whereas leak-before-break involves stable cracking out to the OD followed by extensive cracking along the OD surface before final fast failure. Cannon pressure vessels are best analyzed using yield-before-break methods.

Irwin plastic zone concepts also can help explain an important and common observation associated with fast fracture of cannon tubes, i.e., the tendency for fast fracture to occur at an applied K level somewhat above the critical value of K corresponding to K_{Ic}, the fracture toughness. Recall the earlier results here, where $K_{Ic} = 74$ MPa $m^{1/2}$, contrasted with an applied K at failure of 99 MPa $m^{1/2}$. This is a common observation with fast fracture of cannons, and although it is a beneficial effect, it may not always be present. It is prudent to seek understanding of the effect. Differences in configuration of the fracture toughness compact specimen compared with a pressurized cannon tube are believed to be important.

Table 3 shows an analysis of applied K and plastic zone size for various pressurized tube conditions and makes comparisons with similar conditions for compact specimens. The applied

K for a shallow crack in a pressurized thick tube in the 1.12 (stress) $(\pi c)^{1/2}$ form (ref 1) is used as follows:

$$K_{APL} = 1.12\, fp(\pi c)^{1/2}[(b^2/a^2 + 1)/(b^2/a^2 - 1) + p] \qquad (2)$$

The values used in equation (2) were from the early work (ref 1):

- $f = 0.62$ to account for the semi-elliptical shaped crack
- Applied pressure, $p = 345$ MPa
- Outer- to inner-radius ratio $b/a = 2.10$

Table 3. Effect of Plastic Zone Size on Fracture of Cannons

		Crack Depth (mm)	K_{APL}/K_{Ic}	$c/2.5(K_{Ic}/Y)^2$
K_{Ic} = 74 MPa $m^{1/2}$	Tube:	5	1.05	0.51
Y = 1180 MPa		10	1.48	1.02
		15	1.82	1.53
	Compact:	25	--	2.54
K_{Ic} = 140 MPa $m^{1/2}$	Tube:	15	0.96	0.37
Y = 1100 MPa		20	1.11	0.49
		25	1.24	0.62
	Compact:	25	--	0.62

For the toughness and strength of the early tube, as crack depth, c, increases the applied K soon exceeds the fracture toughness. The reason the failure is delayed is shown by the values of $c/2.5(K_{Ic}/Y)^2$, which, as discussed in relation to equation (1), is the size requirement for plane-strain fracture. In the case here of shallow cracks, the critical dimension is the dimension behind the crack tip, i.e., the crack depth. When the ratio $c/2.5(K_{Ic}/Y)^2$ exceeds 1, a plane-strain fracture is likely. Note that this ratio has reached about 1 at the 10-mm crack depth at which the early fracture occurred. For a compact fracture toughness test of the earlier obsolete gun steel using a 50-mm depth specimen, all critical dimensions, including the crack depth, are about 25-mm. Also, the $c/2.5(K_{Ic}/Y)^2$ value of 2.54 shows that plane-strain fracture is clearly indicated, as our experience has shown.

For the toughness and strength of current tube steel, the situation is quite different. No brittle fast fracture is expected in a cannon tube or in a fracture toughness specimen of typical size. Yield-before-break fractures are observed in modern cannons, and the elastic-plastic J_{Ic} test procedure is required for fracture toughness measurement. The added complexity of the J_{Ic} test is a small price to pay for the safety of yield-before-break behavior in cannon tubes. An example of a yield-before-break cannon failure is shown in Figure 4, the fracture surface of a fatigue life test of the breech-end of a 120-mm cannon tube. Note that the final break-through of the fatigue crack to the tube OD (near top-center of the photo) is small and is accompanied by a large shear lip, which indicates a safe conclusion to the fatigue test. Additional aspects of fatigue fracture in cannon tubes, in addition to the final failure event, are considered next.

Figure 4. Fracture surface of a 120-mm tube section.

FATIGUE FRACTURE

Safe Fatigue Life Tests

The basis for all fatigue life measurements and analysis of Army cannon tubes is the concept of full-size laboratory tests of sections of pre-fired cannons. Figure 4 shows the fracture surface of a breech-end section of a 120-mm tube after the section had been broken apart to reveal the crack surfaces following the test. Starting from the bottom of the photo, the following characteristics are illustrated:

- A portion of the tube ID with severe thermal damage from cannon firing before the fatigue test
- The initiation and growth phases of the semi-elliptical shaped fatigue crack
- The small yield-before-break final fast fracture, already discussed

Apart from a much more severe than normal thermal damage, these features are typical of safe fatigue life tests of cannon tubes. Typically, six cannons are pre-fired in order to produce ID thermal damage typical of expected field conditions, made into 1- to 2-m long sections, and hydraulically fatigue cycled to failure.

The results of safe fatigue life tests are used to determine safe life, N^*, which is calculated in terms of the mean and standard deviation of the natural logs of the test lives, N, as follows (ref 5):

$$N^* = exp[(ln\ N)_{AVE} - k(ln\ N)_{SD}] \qquad (3)$$

where k is the normal distribution tolerance factor for a given confidence that at least a certain proportion of a population will be above the safe life. Table 4 shows example results based on arbitrary values of 90% confidence and 0.99 reliability. Values used for cannon safe lives depend on cannon usage. Note in equation (3) that safe life can be considerably below mean life, particularly for a large standard deviation relative to mean life. This experimentally-based safe fatigue life determination has proven to be a consistently effective method for guaranteeing the reliability of Army cannon tubes for a wide range of field service conditions.

Table 4. Log-Normal Safe Life Analysis for Cannon Tubes

Specimen Number	Measured Life (cycles)	Tolerance Factor	Safe Life (cycles)
#01	13,800	4.24	5,337
#02	10,319	For: 6 tests	
#03	13,067	90% confidence	
#05	10,828	0.99 reliability	
#09	11,252		
#25	8,501		

Fatigue Life Model

Safe fatigue life tests, in addition to providing a measure of cannon reliability, have in recent years been used to develop a fatigue life model. The model (ref 6) uses a new concept called the *fatigue intensity factor* that adds a quantitative measure of material yield strength and initial crack size to the stress parameter in a *log*-stress versus *log*-life description of fatigue life behavior. With these additions, significant improvements in life modeling of cannon tubes are shown. The key expression for a fatigue intensity factor, *FIF*, description of ID-initiated fatigue life of an autofrettaged cannon tube is

$$FIF = S_{LOCAL} \times (Y_{NOM}/Y) \times (a_i/a_{i\text{-}NOM})^{1/6} \tag{4}$$

The effects of yield strength and initial crack size are the second and third terms, accounting for the yield strength of a given vessel if it is different from the nominal yield strength, and for initial crack size of a given vessel if it is different from the nominal initial crack size. The local stress range includes the familiar Lamé ID hoop applied stress and direct pressure effects, discussed in relation to equation (2), and the ID hoop residual stress, accounting for the Bauschinger-reduced compressive strength of the gun steel.

Parker (ref 7) and Troiano et al. (ref 8) have recently provided the analysis methods and the critical materials property data required to determine the Bauschinger-reduced hoop compressive residual stress at the ID of an autofrettaged gun tube. Prior to this recent work, only approximate analyses and materials data limited to one type of gun steel were available. The local stress range of the *FIF* model, including the Bauschinger-reduced compressive strength of cannon steels, is as follows:

$$\Delta S_{LOCAL} = [k_T\, p(b^2/a^2 + 1)/(b^2/a^2 - 1) + p] + S_{h\text{-}ID} \tag{5}$$

where the first term is the applied stress (with stress concentration k_T where applicable) and direct pressure effects mentioned earlier, and $S_{h\text{-}ID}$ is the Bauschinger-affected hoop residual stress at the ID of a tube with autofrettage radius r_Y. The expression for $S_{h\text{-}ID}$ is (ref 7)

$$S_{h\text{-}ID} = \gamma RY[(r_Y^2 - a^2) - 2b^2 \ln(r_Y/a)]/[b^2 - a^2] \tag{6}$$

where γ and R account for the Bauschinger-reduced strength of cannon steel and open-end conditions in a cannon tube, respectively, and the remainder of equation (6) is the ideal Tresca-plane-stress expression for ID hoop residual stress in an autofrettaged tube. For A723 steel (ref 8)

$$\gamma = 1/[\{A(b/a) + B\}EXP[\{C(b/a) + D\}\{(r_Y/a) + E\}] + \{F(b/a) + G\}]$$

$$for\ r_Y/a > 1.5;\ \ b/a > 1.75 \qquad (7)$$

and R, which is material-independent, is (ref)]

$$R = 1.669 - 0.165(b/a) - 0.730n^3 + 1.984n^2 - 1.887n \qquad (8)$$

where n is the degree of autofrettage, i.e., $n = (r_Y - a)/(b - a)$. The constants in equation (7) for A723 steel are:

- A = 0.0816
- B = –0.0562
- C = 1.7519
- D = –7.4597
- E = –1.315
- F = –0.1077
- G = 1.216

Results for other steels are included in Reference 8.

Equations (4) through (8) are used here in an updated example (ref 9) of the fatigue-intensity-factor fatigue life model for autofrettaged cannon tubes. Table 5 and Figure 5 show the example inputs and results. The values of k_T and a_i in Table 5 account for different stress concentration and initial damage conditions in the various types of cannons. For these four groups of cannons Y_{NOM} = 1134 MPa and $a_{i\text{-}NOM}$ = 0.10-mm. The plot of stress range versus N in Figure 5 (on the left) gives a useful description of fatigue lives for a variety of cannon types, with reasonably good correlation, $R^2 = 0.74$. But note the further significant improvement when *FIF* is used (on the right), with $R^2 = 0.92$. This shows the advantage of adding a quantitative measure of material yield strength and initial crack size to the stress parameter in a *log*-stress versus *log*-life model of fatigue life behavior. With this improved description of life, model calculations can be made to show effects of key parameters on fatigue life of cannon tubes. This is considered next.

Table 5. Inputs to Fatigue Life Model

Group	Y (MPa)	n (%)	A (mm)	b (mm)	k_T	a_i (mm)	P (mm)
#1	1280	0	89	187	1.7	0.01	345
#2	1020	50	89	187	1.7	0.01	345
#3	1230	60	89	142	1.0	0.10	393
#4	1120	60	79	155	1.0	0.10	670

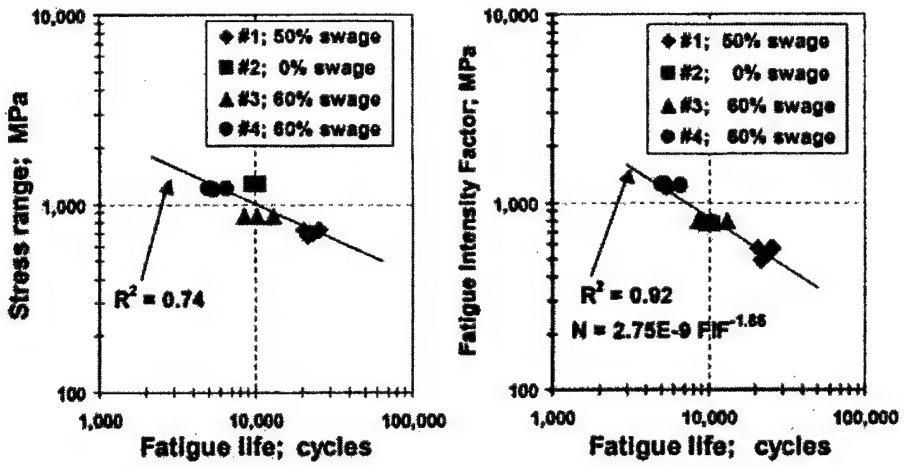

Figure 5. Fatigue life models; *FIF* and stress range.

The regression equation for N in terms of *FIF* shown in Figure 5 can be used to determine the effect of hoop ID residual stress on fatigue life for autofrettaged cannons. Figure 6 shows three plots of calculated life versus fatigue pressure for the group #4 cannon of the preceding discussion. Calculations including Bauschinger-affected residual stress as appropriate for an autofrettaged cannon [determined from equations (6) through (8)] are shown as the solid curve. Also shown are calculations for ideal Tresca-plane-stress residual stresses [with $\gamma = R = 1$ in equation (6)] and calculations with no residual stresses. It is clear that ideal residual stresses give a high, nonconservative estimate of fatigue life and no residual stresses give a low, conservative estimate of life. The lives at the 670 MPa fatigue pressure, at which the group #4 safe life fatigue tests were performed, are shown in Figure 6. The 5570 cycle calculated life, including Bauschinger effects, is in good agreement with the group #4 lives plotted in Figure 5.

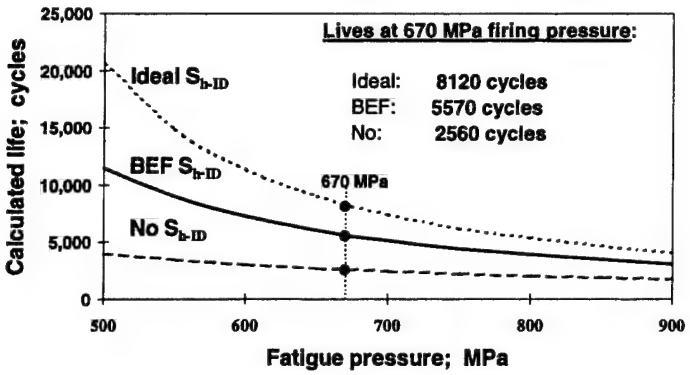

Figure 6. Effect of residual stress on fatigue life.

The fatigue life model described here is quite recently developed (ref 6) and only very recently modified (refs 7,8) to include the appropriate Bauschinger-effect analysis and material properties. It is a proposed tool to complement the complex, experimental, safe-fatigue-life tests that have long been used and will continue to be used for Army cannons.

ENVIRONMENTAL FRACTURE

Two of the classic trios of requirements for environment-assisted fracture have always been present in cannon tubes—the aggressive environment and the susceptible material. Hydrogen is a major component of cannon gases, and the high-strength, martensitic cannon steels are highly susceptible to many environments, certainly including hydrogen. Unfortunately, the third requirement for environmental fracture—a sustained tensile stress—is becoming more prevalent in today's cannons than those of the past. The source of this tensile stress is more extensive ID thermal damage, due to higher and more prolonged cannon gas temperatures. The connection between thermal damage, sustained tension, and hydrogen cracking is the subject of a companion paper (ref 10) to this review, so only a few key results will be given here.

The general types of thermal damage that occur near the ID surface of a fired cannon and near the surface of a laser-heated laboratory specimen used to simulate cannon firing (ref 11) are contrasted in Figure 7. The fired cannon has the usual electroplated chromium coating, typically 0.1-mm thick. The laser-heated specimen has a sputtered chromium coating nearly as thick. The thermal damage in the two types of heated sample have many things in common, including cracking and recrystallization plus grain growth in the chromium and phase transformation in the steel. However, it is clear that only the cannon fired sample has significant cracking in the steel beneath the chromium. This, in combination with the crack morphology and the known presence of hydrogen in cannon gases, suggests that hydrogen is the cause of near-bore environmental cracking in cannon firing. The laser-heated sample was exposed to no more than trace hydrogen, and thus the steel did not crack. A series of laboratory hydrogen cracking tests (ref 12) has been performed to help verify that hydrogen contributes to firing damage. Hydrogen cracking in the near-bore region of a cannon can be further verified by a thermomechanical analysis of the near-bore region of a fired tube, considered next.

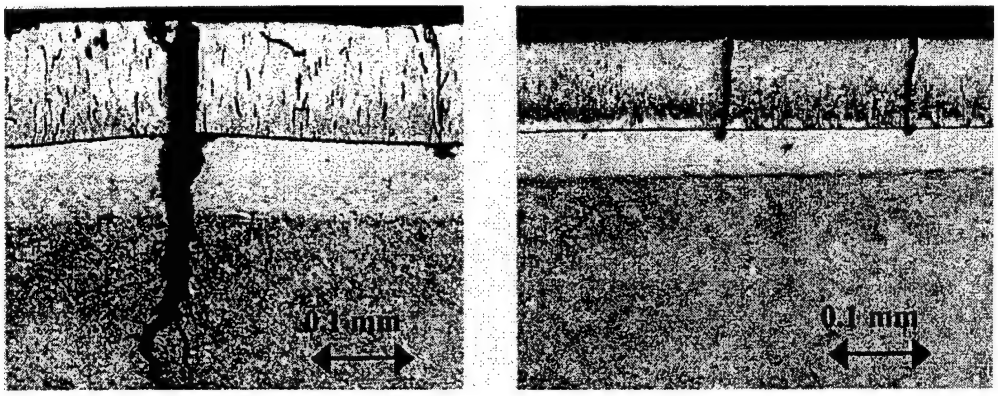

(a) cannon firing (b) laser heating

Figure 7. Thermal damage and cracking in fired tube and laser-heated specimen.

An initial model of the transient thermal firing stresses and their environmental fracture consequences (ref 13) has been taken further in the companion paper to this, already mentioned (ref 10). Figures 8 and 9 show results of this thermomechanical modeling for the two examples shown in Figure 7. The plots for cannon firing and laser heating are fundamentally the same. In both Figures 8 and 9 temperatures from finite-difference calculations are validated by the known 1020°K steel transformation temperature and are also in reasonable agreement with the 1320°K grain growth temperature for chromium. Using these temperatures the near-bore, transient, biaxial compressive thermal stress, S_T, and the tensile residual stress, S_R, produced in the steel substrate when the transient stress exceeds the steel yield strength, are as follows:

$$S_T = -E\alpha[T\{x,\Delta t\} - T_i]/[1 - \nu] \tag{9}$$

$$S_R = -S_T - Y \qquad for\ S_T > Y \tag{10}$$

where E and α are temperature-dependent elastic modulus and expansion coefficient, respectively; the transient temperature, $T\{x,\Delta t\}$ from the finite-difference calculations is for a given depth, x, below the bore surface and duration, Δt, of a heating pulse; the term $[1 - \nu]$ accounts for the biaxial nature of the temperature and stress distributions.

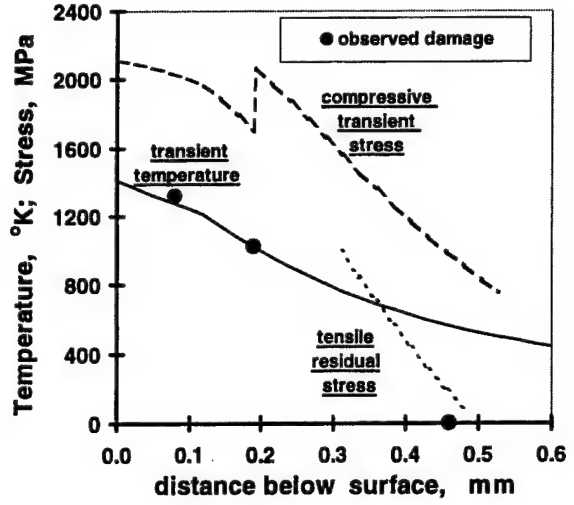

Figure 8. Thermomechanical model for near-bore thermal damage and cracking in fired cannon #26.

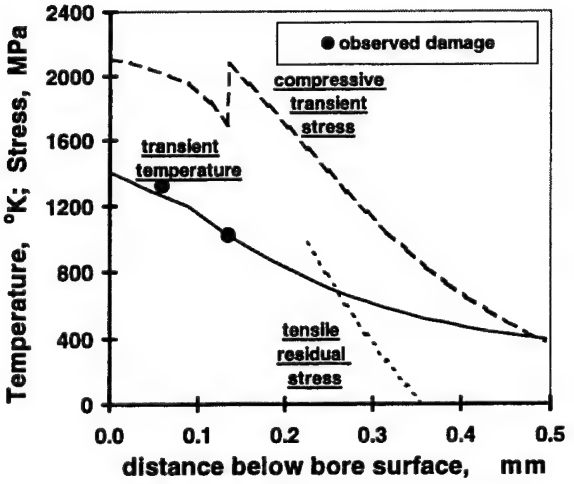

Figure 9. Thermomechanical model for near-surface thermal damage and cracking in a laser-heated sample.

The transient compressive stress plotted in Figures 8 and 9 at large distances below the surface, thus at lower temperatures, is due only to thermal expansion. However, at 1020°K, the 0.25% contraction (ref 13) due to the martensite-to-austenite phase transformation has been added in the work here. Note that the effect of this contraction on the transient compressive stress is quite small compared to that of the thermal expansion, and the net result is a compressive stress that remains well above the yield strength of the steel. Also, the deepest depth at which the *transient compressive* stress is above the yield strength determines the depth of the *residual tensile* stress after cooling. This is the sustained tensile stress that drives the near-bore hydrogen cracks in fired cannons. Note the good agreement between calculated depth of

tensile residual stress (0.50-mm) and observed crack depth (0.46-mm) in Figure 8. For the laser-heated sample, a significant depth of residual stress was calculated, but no hydrogen was present and no cracks were observed, as has been discussed.

The thermomechanical model of near-bore temperatures and stresses discussed here agrees well with observations in both fired cannons and laboratory simulations of firing. It will continue to be used to describe cannon firing damage and to help develop improved cannon bore protective coatings to minimize firing damage. The interrelation of thermal-damage driven cracking with bore coatings is considered next.

COATING FRACTURE

The comprehensive review of thermomechanical integrity of thin coatings by Evans and Hutchinson (ref 14), particularly their slip-zone concept, is adapted here and in a companion paper (ref 10) to predict fracture strength of cannon bore coatings. As in the prior discussion of environmental fracture, coating fracture is controlled by the thermal damage associated with cannon firing. The thermal damage shown in Figure 7 for actual and simulated cannon firings is a useful example of coating fracture processes. The key concepts of the Evans/Hutchinson slip-zone model, as adapted to fracture of cannon coatings, are shown in Figure 10.

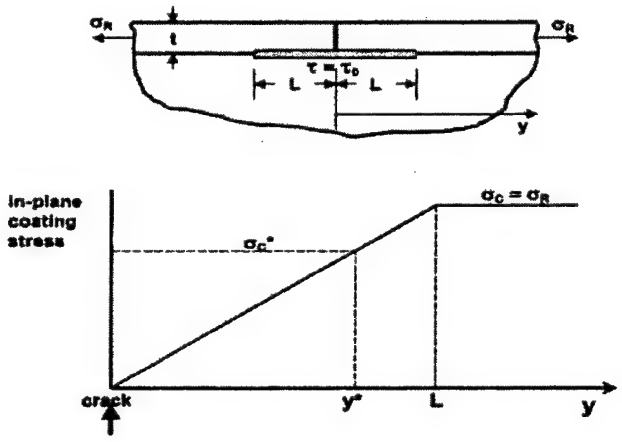

Figure 10. Interface-slip-zone model for coating fracture.

A schematic of a section of coating and substrate is illustrated in Figure 10, with a tensile residual stress, S_R, in the coating of thickness, t. The source of residual stress is the thermal damage process described earlier. When the residual stress is relieved at a preexisting crack site, the load formerly carried by the coating is then carried by a shear zone of length, L, on either side of the crack.

An expression for the tensile residual stress in terms of the minimum shear yield strength near the interface, τ_0, and dimensions t and L from Figure 10 is

$$S_R t = \tau_0 L \qquad (11)$$

Using this expression and the concept (plot in Figure 10) that the in-plane tensile stress in the coating increases linearly with distance, y, away from the crack location, leads to

$$y^*/t = S_C^*/\tau_0 \qquad (12)$$

where y^* is the critical crack spacing away from a preexisting crack at which the coating stress reaches the tensile failure strength of the coating material, S_C^*. The use of equation (12) in the examples of Figure 7 is summarized in Table 6. The observed crack spacing in the coating (from photos such as Figure 7) and the measured minimum shear strength near the interface (from microhardness measurements) provide a measure of the tensile failure strength of the coating. Note that the tensile fracture strength for sputtered chromium is more than twice that of electroplated chromium, a clear advantage for protecting the cannon bore.

Table 6. Coating Characterization and Failure Strength

Coating	Coating Thickness (t, mm)	Crack Spacing (y^*/t)	Shear Strength (τ_0, MPa)	Failure Strength (S_C^* MPa)
Chromium Electroplate *Cannon Firing*	0.12	1.2	580	700
Chromium Sputtered *Laser Heating*	0.09	2.5	700	1730

Coating fracture results of this sort have particular value because they are in-situ measurements of coating strength under the actual thermal damage conditions that first modify the coating properties and then apply the thermal loading to the modified coating. The work in Reference 10 and that summarized here is a new type of fracture modeling for thermally damaged coatings. It is believed to have particular applicability to the ongoing development of bore protective coatings for U.S. Army cannons.

SUMMARY

Fast fracture in cannon tubes is well described using the elastic-plastic fracture toughness properties of cannon steels, in combination with critical comparisons of cannon section size relative to the size required to maintain plane-strain fracture test conditions.

Fatigue fracture of cannon tubes can be reliably described and modeled from the results of full-size laboratory fatigue tests that simulate cannon firing. Such tests also form the experimental basis of *fatigue intensity factor* modeling of fatigue life, which incorporates material strength, initial crack size, and Bauschinger-modified autofrettage residual stress effects into fatigue life predictions.

Environment-assisted fracture in the thermally damaged near-bore region of fired cannons has been found to be controlled by hydrogen. High-strength cannon steels are susceptible to hydrogen, the hydrogen environment is provided by cannon gases, and the sustained tensile stress is created from thermal expansion leading to compressive yielding. Thermomechanical modeling predicts tensile residual stress of similar depth to that of observed hydrogen cracks.

Coating fracture in the thermally damaged near-bore region of fired cannons has recently been characterized and modeled. The Evans/Hutchinson slip-zone is adapted to calculate in-situ coating fracture strength based on observed crack spacing and microhardness in the damaged region.

REFERENCES

1. Davidson, T.E., Throop, J.F., and Underwood, J.H., "Failure of a 175mm Tube and the Resolution of the Problem Using an Autofrettaged Design," *Case Studies in Fracture Mechanics*, (T.P. Rich and D.J. Cartwright, eds.), Army Materials and Mechanics Research Center, Watertown, MA, 1977, pp. 3.9.1-13.

2. "Standard Test Method for Measurement of Fracture Toughness," ASTM E1820, *Annual Book of ASTM Standards*, Vol. 03.01, American Society for Testing and Materials, West Conshohocken, PA, 2000, pp. 1000-1033.

3. "Standard Test Methods E23 for Notched Bar Impact Testing of Metallic Materials," ASTM E23, *Annual Book of ASTM Standards*, Vol. 03.01, American Society for Testing and Materials, West Conshohocken, PA, 2000, pp. 138-162.

4. Underwood, J.H., Farrara, R.A., and Audino, M.J., "Yield-Before-Break Fracture Mechanics Analysis of High Strength Steel Pressure Vessels," *Journal of Pressure Vessel Technology*, Vol. 117, 1994, pp. 79-84.

5. Underwood, J.H., and Audino, M.J., "Effects of Initial Cracks and Firing Environment on Cannon Fatigue Life," *Fatigue Design 1998, Vol. II*, Technical Research Centre of Finland, Espoo, Finland, 1998, pp. 491-500.

6. Underwood, J.H., and Parker, A.P., "Fatigue Life Assessment of Steel Pressure Vessels with Varying Stress Concentration, Residual Stress and Initial Cracks," *Advances in Fracture Research, Proceedings of ICF9,* Pergamon, 1997, pp. 215-226.

7. Parker, A.P., "Autofrettage of Open-End Tubes – Pressures, Stresses, Strains and Code Comparisons," *Journal of Pressure Vessel Technology*, Vol. 123, 2001, pp. 271-281.

8. Troiano, E., Parker, A.P., Underwood, J.H., and Mossey, C., "Experimental Data, Numerical Fit and Life Approximations Relating to the Bauschinger Effect in High Strength Armament Steels," *Proceedings of Gun Tubes 2002*, 15-18 September 2002, Oxford, England, in press.

9. Underwood, J.H., Parker, A.P., Troiano, E., Vigilante, G.N., and Witherell, M.D., "Fatigue and Hydrogen Cracking in Cannons with Mechanical and Thermal Residual Stress," *Advances in Fracture Research, Proceedings of ICF10,* Pergamon, 2001.

10. Underwood, J.H., Parker, A.P., Vigilante, G.N., and Cote, P.J., "Thermal Damage, Cracking and Rapid Erosion of Cannon Bore Coatings," *Proceedings of Gun Tubes 2002*, 15-18 September 2002, Oxford, England, in press.

11, Cote, P.J., Kendall, G., and Todaro, M.E., "Laser Pulse Heating of Gun Bore Coatings," *Surface and Coatings Technology*, Vol. 146-147, 2001, pp. 65-69.

12. Vigilante, G.N., Underwood, J.H., Crayon, D., Tauscher, S.S., Sage, T., and Troiano, E., "Hydrogen-Induced Cracking Tests of High-Strength Steels and Nickel-Iron Base Alloys Using the Bolt-Loaded Specimen," *Fatigue and Fracture Mechanics, ASTM STP 1321*, 1997, pp. 602-616.

13. Underwood, J.H., Parker, A.P., Cote, P.J., and Sopok, S., "Compressive Thermal Yielding Leading to Hydrogen Cracking in a Fired Cannon," *Journal of Pressure Vessel Technology,* Vol. 121, 1999, pp.116-120.

14. Evans, A.G., and Hutchinson, J.W., "The Thermomechanical Integrity of Thin Films and Multilayers," *Acta Metallurgica et Materialia*, Vol. 43, 1995, pp. 2507-2530.

TECHNICAL REPORT INTERNAL DISTRIBUTION LIST

	NO. OF COPIES
TECHNICAL LIBRARY ATTN: AMSTA-AR-CCB-O	1
TECHNICAL PUBLICATIONS & EDITING SECTION ATTN: AMSTA-AR-CCB-O	3
PRODUCTION PLANNING & CONTROL DIVISION ATTN: AMSTA-WV-ODP-Q, BLDG. 35	1

NOTE: PLEASE NOTIFY DIRECTOR, BENÉT LABORATORIES, ATTN: AMSTA-AR-CCB-O OF ADDRESS CHANGES.

TECHNICAL REPORT EXTERNAL DISTRIBUTION LIST

	NO. OF COPIES
DEFENSE TECHNICAL INFO CENTER ATTN: DTIC-OCA (ACQUISITIONS) 8725 JOHN J. KINGMAN ROAD STE 0944 FT. BELVOIR, VA 22060-6218	2
COMMANDER U.S. ARMY ARDEC ATTN: AMSTA-AR-WEE, BLDG. 3022 AMSTA-AR-AET-O, BLDG. 183 AMSTA-AR-FSA, BLDG. 61 AMSTA-AR-FSX AMSTA-AR-FSA-M, BLDG. 61 SO AMSTA-AR-WEL-TL, BLDG. 59 PICATINNY ARSENAL, NJ 07806-5000	 1 1 1 1 1 2
DIRECTOR U.S. ARMY RESEARCH LABORATORY ATTN: AMSRL-DD-T, BLDG. 305 ABERDEEN PROVING GROUND, MD 21005-5066	 1
DIRECTOR U.S. ARMY RESEARCH LABORATORY ATTN: AMSRL-WM-MB (DR. B. BURNS) ABERDEEN PROVING GROUND, MD 21005-5066	 1
CHIEF COMPOSITES & LIGHTWEIGHT STRUCTURES WEAPONS & MATLS RESEARCH DIRECT U.S. ARMY RESEARCH LABORATORY ATTN: AMSRL-WM-MB (DR. BRUCE FINK) ABERDEEN PROVING GROUND, MD 21005-5066	 1

	NO. OF COPIES
COMMANDER U.S. ARMY RESEARCH OFFICE ATTN: TECHNICAL LIBRARIAN P.O. BOX 12211 4300 S. MIAMI BOULEVARD RESEARCH TRIANGLE PARK, NC 27709-2211	 1
COMMANDER ROCK ISLAND ARSENAL ATTN: SIORI-SEM-L ROCK ISLAND, IL 61299-5001	 1
COMMANDER U.S. ARMY TANK-AUTMV R&D COMMAND ATTN: AMSTA-DDL (TECH LIBRARY) WARREN, MI 48397-5000	 1
COMMANDER U.S. MILITARY ACADEMY ATTN: DEPT OF CIVIL & MECH ENGR WEST POINT, NY 10966-1792	 1
U.S. ARMY AVIATION AND MISSILE COM REDSTONE SCIENTIFIC INFO CENTER ATTN: AMSAM-RD-OB-R (DOCUMENTS) REDSTONE ARSENAL, AL 35898-5000	 2
NATIONAL GROUND INTELLIGENCE CTR ATTN: DRXST-SD 2055 BOULDERS ROAD CHARLOTTESVILLE, VA 22911-8318	 1

NOTE: PLEASE NOTIFY COMMANDER, ARMAMENT RESEARCH, DEVELOPMENT, AND ENGINEERING CENTER, BENÉT LABORATORIES, CCAC, U.S. ARMY TANK-AUTOMOTIVE AND ARMAMENTS COMMAND, AMSTA-AR-CCB-O, WATERVLIET, NY 12189-4050 OF ADDRESS CHANGES.